CONICAL SCANNING SYSTEM

FOR

PIONEER JUPITER SPACECRAFT

V. Z. Viskanta and R. E. Rose
TRW Systems Group

ABSTRACT

In this paper the concept, operation and predicted performance of the RF tracking control system used to point the Pioneer F/G spacecraft at the earth is described. This system employs modified conical scanning technique and is referred to as Conscan.

The spin of the spacecraft produces amplitude modulation of the uplink communication signal when the spacecraft antenna is offset in pointing from the spin axis. This modulation is detected via a receiver AGC loop. The phase and amplitude of the modulation (or Conscan signal) are then used to determine the direction of the earth line from the spin axis and the magnitude of the angle (pointing error) between them. A digital signal processor is employed to measure the phase and amplitude of the Conscan signal. The phase information is used to issue firing pulses to precess the spacecraft to a new pointing direction while the amplitude, which is proportional to the pointing error angle, is needed to terminate the maneuver when the spin axis is within some preselected pointing angle from the earth.

The signal processor is the most interesting unit of the system and is described and analyzed in detail to show that it approximates maximum likelihood estimator. The dynamic behavior of the spacecraft and the stability analysis of the system is presented demonstrating that the system performance is basically determined by the open loop phase and amplitude error introduced by the antenna, receiver and the signal processor. A detailed error budget is included to show that the phase and amplitude errors are small. Finally, a summary of the closed loop simulation and test data is presented to verify that the error budget is realistic.

I. INTRODUCTION

The Pioneer F/G spacecraft being built by TRW Systems Group for NASA is scheduled for launch in March 1972 and will be the first mission to explore Jupiter. It will also be the first spacecraft having a "Conscan" closed loop attitude control system for pointing the high gain antenna at earth. This attitude control system uses a conical scanning angle tracking technique described in this paper. In the following sections a complete system description including implementation, closed loop dynamics and performance is presented.

A dominant characteristic of the Jupiter mission is the extreme communication distance and the cost of raw power for signal transmission. To obtain the required telemetry and command capability, a 9-foot antenna which can be accurately pointed is used for Pioneer F/G. One practical technique available to achieve accurate pointing is to implement an RF-angle tracking system. With the spin stabilized spacecraft, a conical scanning (Conscan) angle tracker can be simply implemented since the scanning is automatically provided when the antenna pattern center of symmetry is offset from the spacecraft spin axis.

Figure 1 is a drawing of the spacecraft which illustrates the location of the antennas and the precession thrusters. The main physical feature of the spacecraft is the parabolic antenna reflector which has a tripod support for the high gain antenna feed, feed movement mechanism and the medium gain horn.

The basic Conscan technique described here is frequently employed with ground and airborne radars. However, the overall implementation of the Pioneer Jupiter attitude control system is appreciably different from the common Conscan radars. These implementation differences cannot be easily summarized, but should become clear from the description presented in Section II.

The operation of the Pioneer Conscan system, in many respects, is similar to the angular acquisition of a target with a conventional angle tracking radar. In our case, after the earth (target) is acquired, the Conscan operation is automatically terminated and can be initiated only be a ground command. Due

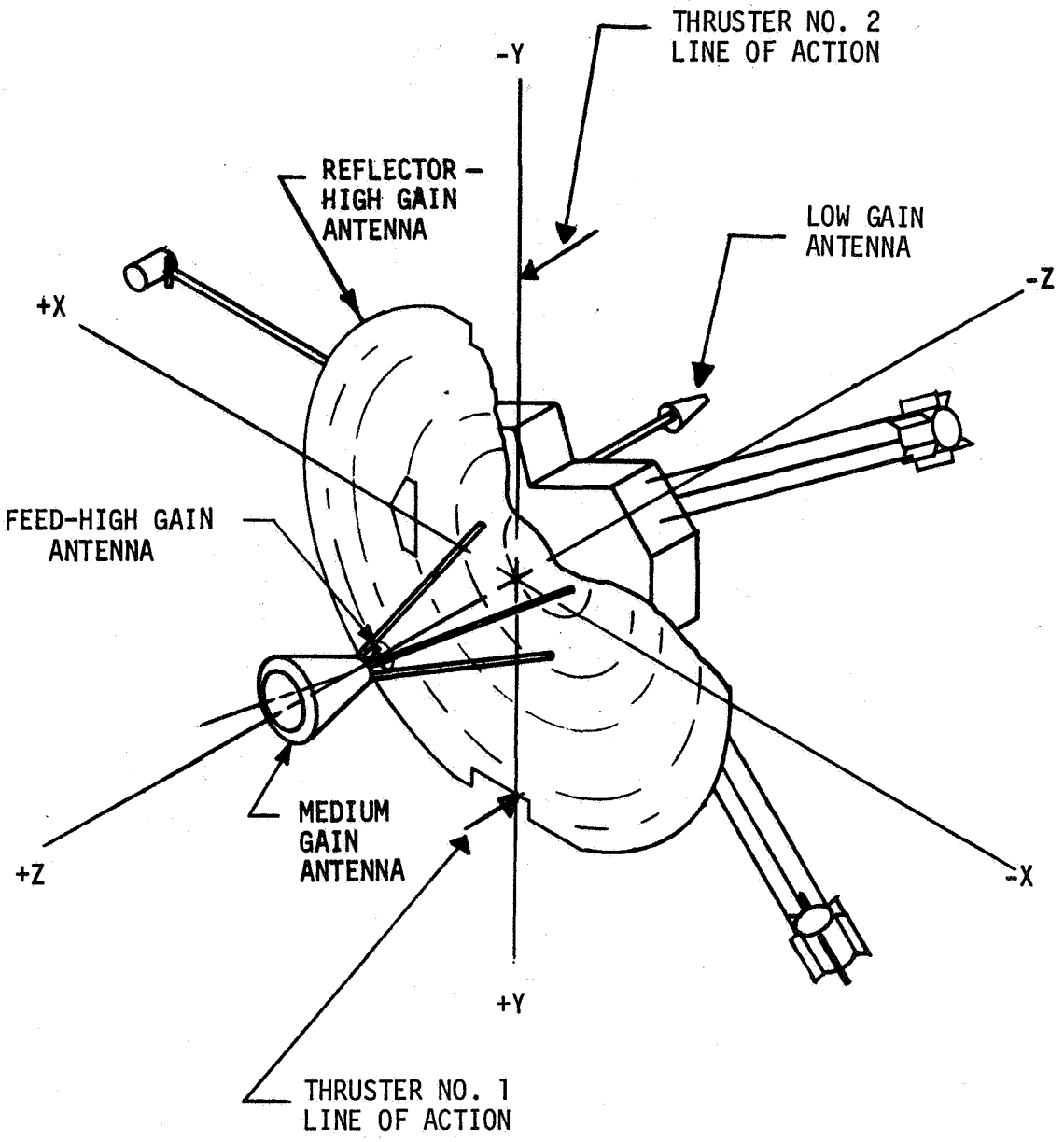

FIGURE 1. SPACECRAFT CONFIGURATION

7

to the motion of the earth and the spacecraft drift, conscanning has to be repeated every few days (sometimes less frequently) throughout the mission. The intermittent operation not only conserves attitude control fuel, but the expensive deep space station transmitter used as a beacon does not have to operate continuously.

This paper is organized as follows: Section II presents a general system description, while Section III provides detailed signal processor description and analysis. Section IV discusses stability considerations. In Section V a performance assessment is presented including error budget and examples of experimental results.

II. SYSTEM DESCRIPTION

The Pioneer spacecraft Conscan system shown in Figure 2 is a closed loop attitude control system for aligning the spacecraft spin axis and, therefore, the body fixed antenna with an RF signal from the earth. This control system can be best described as an impulse controller. The conscanning operation starts at a large pointing angle and a known precession step size and terminates when the deadzone is reached.

The Conscan system is implemented by offsetting the antenna radiation pattern from the spacecraft spin axis. Due to this offset, as the spacecraft spins (at approximately 4.8 R.P.M.), the uplink RF carrier received from the ground station is amplitude modulated. The amplitude modulation is the error signal and is detected by the receiver automatic gain control (AGC) and the Conscan processor. The amplitude of this error signal is approximately proportional to the pointing error angle and is used to terminate Conscan when a preset deadzone has been reached, while the phase provides the timing pulse for the thruster firing. It should be emphasized that only two additional units - the feed movement mechanism and signal processor, are required to implement the Conscan system other than those normally used for communication and open loop attitude control.

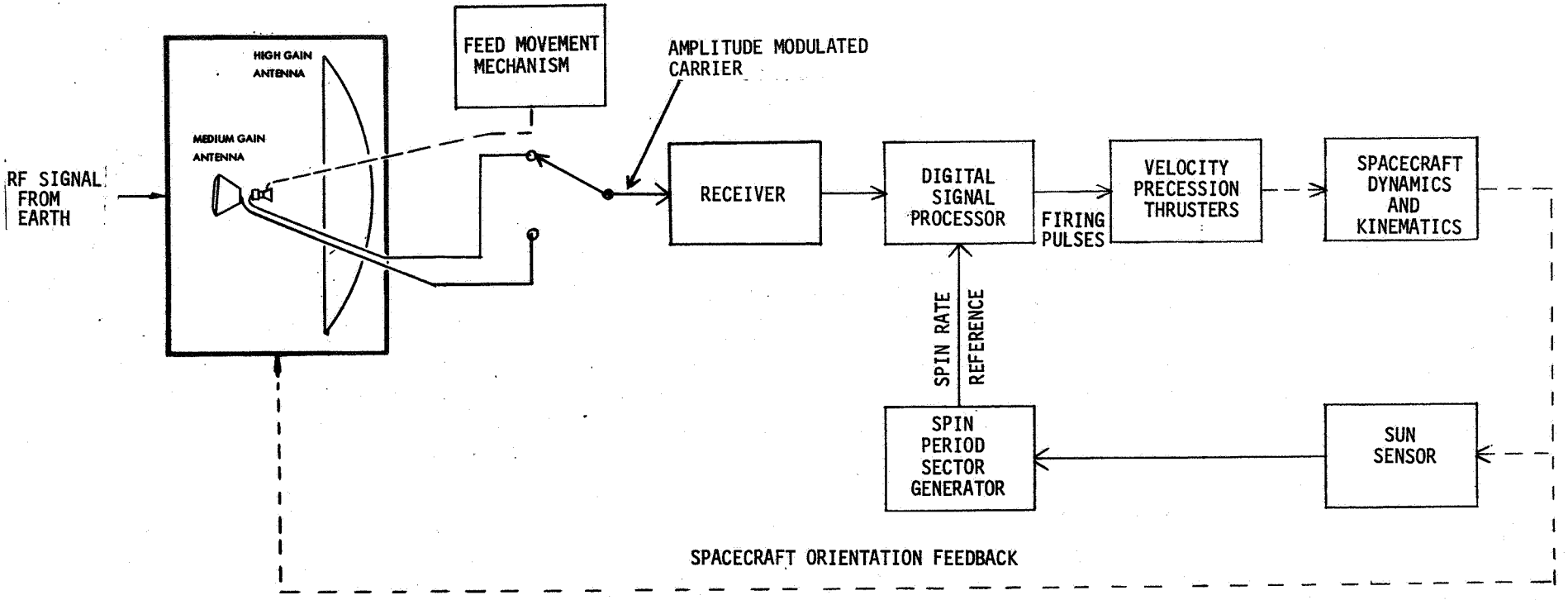

FIGURE 2. SIMPLIFIED CONSCAN SYSTEM BLOCK DIAGRAM

As shown in the block diagram, two antennas are available for Conscan operation. The medium gain antenna is a corrugated horn and is required for acquisition and coarse scanning. The circumferential slots on the horn interior suppress the backlobe level and thus minimize ripple due to interferometer effects caused by reflections from the high gain dish. The medium gain antenna is permanently tilted 9.3 degrees from the spin axis, producing a crossover level of 1 dB. The choice of this crossover level is a compromise between optimum Conscan performance and communication coverage requirements. The 3 dB beamwidth is about 32 degrees and therefore this antenna could be used to acquire the earth within 20 degrees of the spin axis. To minimize propellant consumption, and operational costs, a deadzone for the medium gain antenna of 1.3 degrees has been selected.

The high gain antenna consists of a 9-foot parabolic reflector with a crossed dipole feed located at the focus. For normal telemetry transmission, the high gain antenna pattern is parallel to the spin axis and is only tilted by about 1 degree (1 dB crossover) when the fine Conscan is required. The high gain antenna provides a pencil beam pattern of about 3.5 degrees beamwidth and can be used for Conscan for pointing angles from at least 2.5 degrees to nominal deadzone of 0.3 degrees. The tilting of the antenna beam is accomplished by mechanically offsetting the feed from the focus with the feed movement mechanism. The mechanism incorporates a thermal actuator which upon ground command, mechanically displaces the feed approximately 1 inch along the -Y axis.

The amplitude modulated antenna output is coherently detected by the receiver AGC which provides about 70 dB of dynamic range with linearity exceeding $\pm$ 10 percent. The AGC is primarily required to remove Conscan signal amplitude dependence on the received carrier power level which varies with the communications distance. To simplify AGC loop design and to reduce Conscan signal harmonic interference, wideband AGC with about 1.8 Hz 3 dB bandwidth was selected.

The main function of the signal processor is to estimate the phase and the amplitude of the Conscan signal embedded in noise and interference produced by wobble and antenna pattern distortion. The phase, or the zero axis crossing information, is used to time the precession thruster firing so that the pointing error is reduced with minimum expenditure of propellant. The amplitude

information, which is proportional to the pointing error, is used to terminate the thruster firing when the deadzone has been reached. The selected digital implementation of the processor approximates an optimum maximum likelihood phase and amplitude estimator. An important characteristic of this implementation is the need for an accurate spin rate or frequency reference. In this application this reference is supplied by the sun sensor. While the use of the spin rate reference results in a simpler and more optimum processing, the complexity of the overall system is somewhat increased by the second loop as shown in Figure 2. It is important to point out that the signal processing does not require a phase reference, but does require that the phase be stable during the computation period of 3 revolutions. The choice of the digital versus analog implementation was easy since with the extremely low Conscan frequency of 0.08 Hz, the digital implementation is simpler and results in improved response, stability, and reliability.

The spin rate reference to the signal processor is supplied by the spin period sector generator (SPSG). The SPSG is referenced from the sun sensor which is used as an attitude reference*. The SPSG counts an internal clock for one spacecraft revolution (time between sun pulses) and digitally divides this number into 512 evenly spaced sectors. These timing signals are primarily used for the scientific instruments and for the open-loop attitude control maneuvers; however, they are also suitable to provide timing to the Conscan processor. The SPSG has another mode of operation in which the reference frequency is based on the period of the previous 64 revolutions. This mode of operation reduces the effect of phase jitter due to wobble.

The firing pulses from the signal processor are applied to the spacecraft precession thruster pair. This pair consists of thruster No. 1 located on the +Y axis with the throat facing +Z direction and thruster No. 2 located on -Y axis with the throat facing -Z direction. The application of the firing

---

* The sun sensor produces a single pulse on each revolution of the spacecraft when the sun intersects the Y, Z plane on the +Y side of the spacecraft. The one pulse per revolution signal is the "roll reference pulse" used by the SPSG.

pulses to this thruster pair produces a torque impulse. The torque impulse causes a change in the direction of the angular momentum vector and precesses the spin axis in the direction of the -X axis at the instant of pulse firing by a constant amount, the precession step size. Since the pulses are narrow (125 ms or 31.25 ms) relative to the rotation period of 12.5 seconds, the applied torque can be considered as an impulse.

The firing of the thrusters also induces a wobble or nutational motion of the spin axis about the angular momentum vector. As shown in Appendix A, there are two sinusoidal wobble terms at frequencies 1.85 ω_s and 0.15 ω_s (ω_s is the spin frequency in rad/s). The higher frequency term is by far the larger in amplitude and is slightly less than the precession step size. When computing system errors, the two wobble terms can be approximated by an additive interference. Fortunately, because the wobble frequencies are far removed from the Conscan frequency, most of the interference due to wobble is filtered out by the signal processor.

As discussed in Appendix A, the wobble amplitude depends on the frequency of pulsing or the number of revolutions per precession step, r. For $r > 4$, the maximum wobble amplitude becomes a sensitive function of the spacecraft mass properties and theoretically can grow without bound for some circumstances. To minimize wobble amplitude and variation with mass properties, $r = 3$ was selected. Note that with simple signal processor implementation, as discussed in the following section, the choice of r also specifies the equivalent noise bandwidth. Selection of $r = 3$ results in a reasonable compromise between wobble and the thermal noise performance.

III. SIGNAL PROCESSOR PERFORMANCE

The most important and interesting Conscan system unit is the signal processor. For this reason, in this section it is described and analyzed in detail.

The block diagram of the implemented digital Conscan signal processor is shown in Figure 3. This processor closely approximates the optimum maximum likelihood phase and amplitude estimator of Figure 4.

The analog-to-digital converter samples at the rate of 128 samples per second and uses the successive approximation technique to encode each sampled value to an 8-bit binary word. The data is then mixed with an in-phase and quadrature square wave reference signal and accumulated for two spacecraft revolutions. The two accumulator outputs Acos θ and Asin θ are input into the comparator where the absolute value of the larger, $|L|$, and the smaller, $|S|$, are computed. The amplitude is estimated by the computation algorithm $\hat{A} = |L| + 1/2\ |S|$ and results in a maximum approximation error of $\pm$ 6 percent. In the amplitude comparator, the threshold setting for automatic Conscan termination is selected and the bias type error is compensated.

The phase estimation starts by computing the ratio $|\frac{S}{L}|$ in the divider which is equal to tan θ for $|\cos\theta| > |\sin\theta|$ and to $\cos\theta$ for $|\sin\theta| > |\cos\theta|$. The approximate computation of $\hat{\theta}$ from $\tan\theta$ takes place in the phase counter which counts at a nonlinear rate such that an approximation to the tangent function is generated. The output of the phase counter is compared with the computed $|\frac{S}{L}|$ parameter and a pulse is generated when they are equal. The use of the approximate phase computation algorithm results in maximum error of $\pm$ 2.5 degrees which is negligibly small. When the Conscan signal amplitude is above threshold, a firing pulse is generated to the spacecraft precession thrusters.

The primary function of the Conscan signal processor is to reject both narrowband and wideband (noise) interference and, therefore, reduce phase and amplitude errors. The processor performance with narrowband sinusoidal interference is best illustrated by the frequency response, while the noise performance can be expressed directly in terms of the phase and amplitude errors.

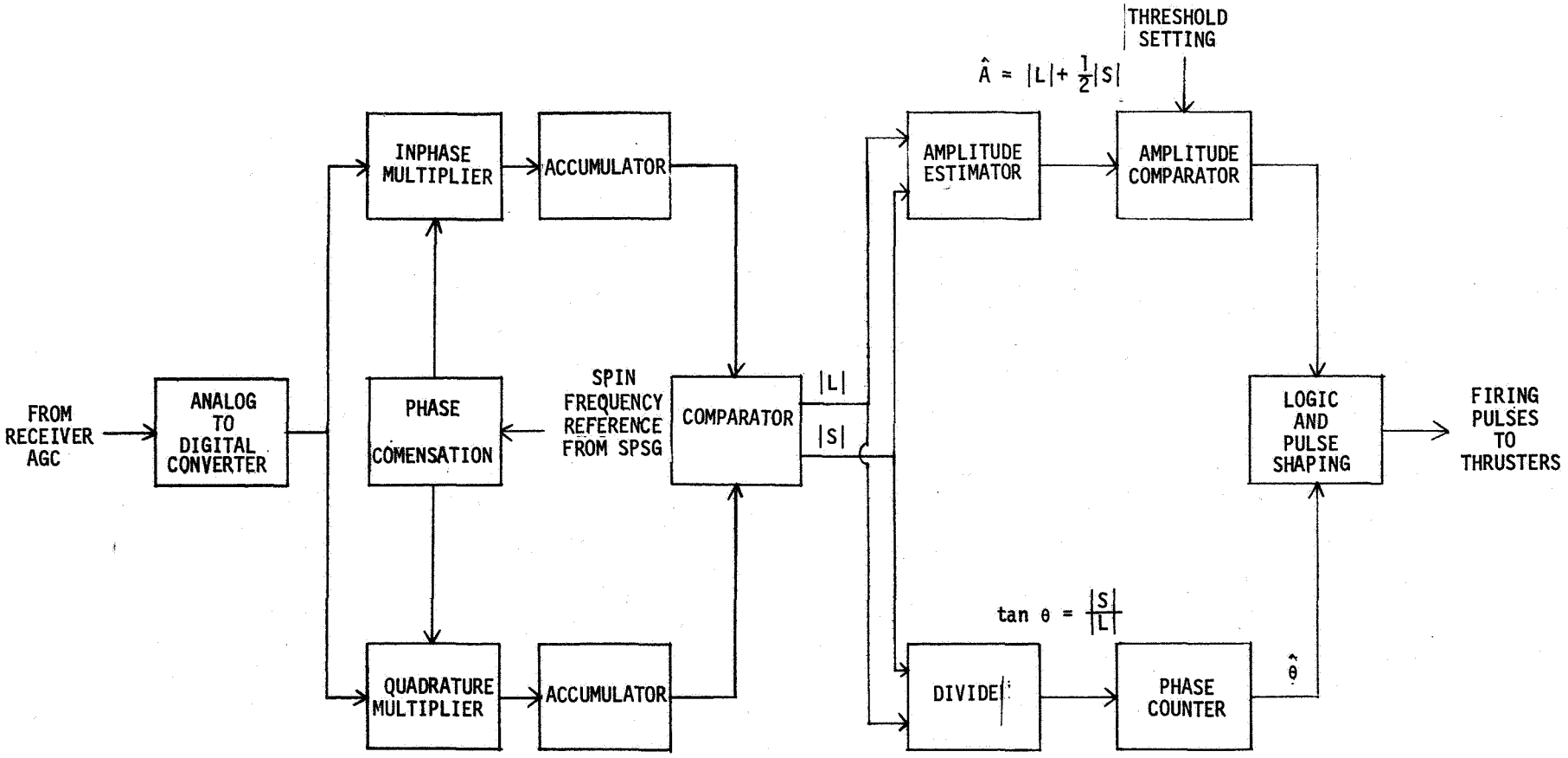

FIGURE 3. SIMPLIFIED SIGNAL PROCESSOR BLOCK DIAGRAM

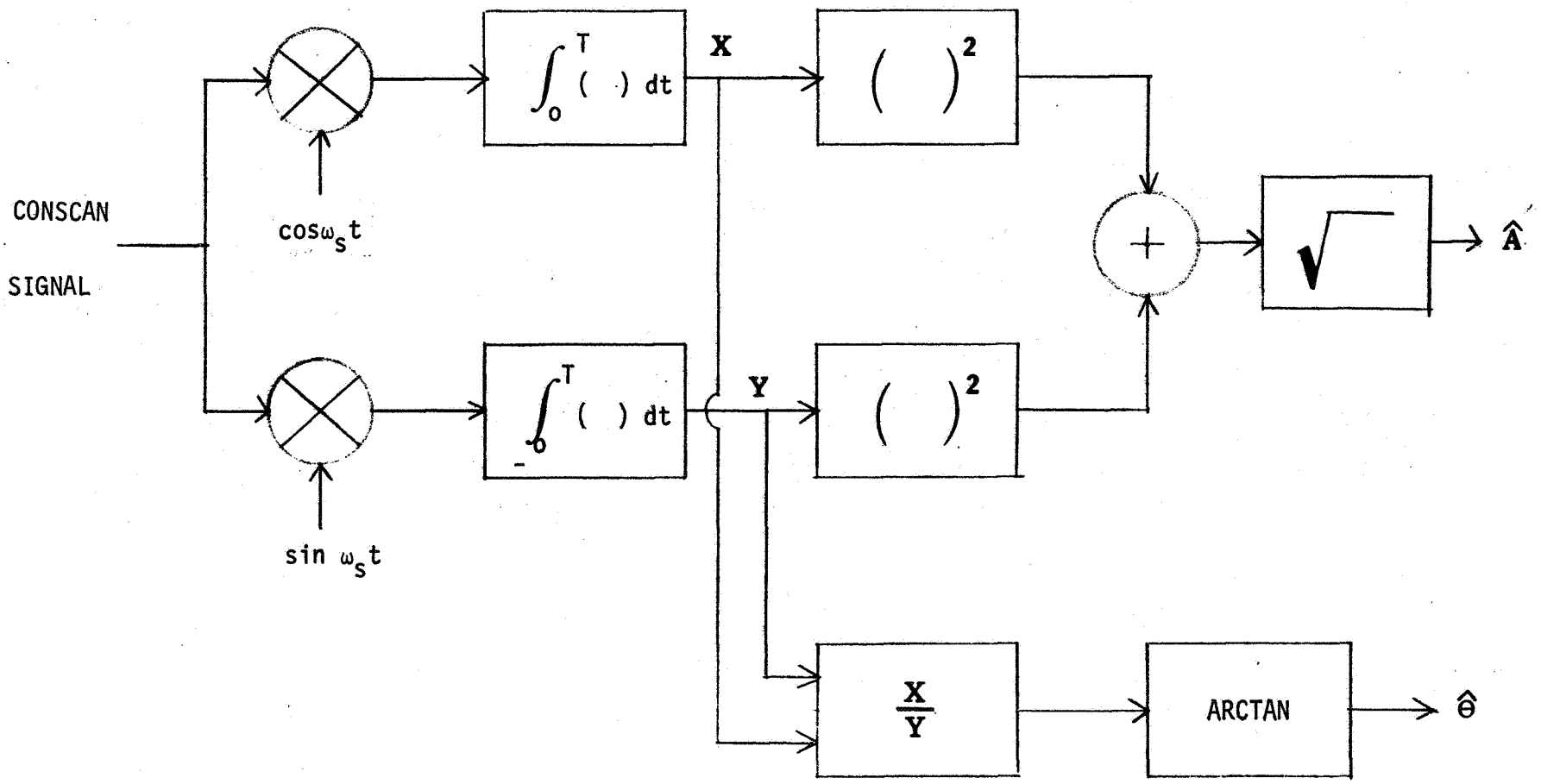

FIGURE 4. MAXIMUM LIKELIHOOD PHASE AND AMPLITUDE ESTIMATORS

Since the filtering in the processor is accomplished by the integrate and dump devices, ideally we would get the well known $|\frac{\sin x}{x}|$ frequency response. However, the multiplier reference signals are square waves, not sinusoids and therefore introduce odd harmonics, $n\omega_s$, of relative amplitude $\frac{1}{n}$.

As far as noise performance is concerned, one might expect that the actual processor can be approximated by the maximum likelihood phase estimator of Figure 4. For this estimator, it has been shown that the lower bound on the variance of the estimated phase is given by [1,2].

$$\text{var}(\theta) = \sigma_\theta^2 \geq \frac{[1+b'(\theta)]^2}{2T\frac{S}{\Phi}} \tag{1}$$

where $b'(\theta)$ is the bias term, S/Φ is the input power-to-noise density and T is the integration time. For high post detection SNR, such as encountered in this application, $b'(\theta) << 1$ and the mean square phase error can be approximated by

$$\sigma_\theta = \left[\frac{\pi^2}{8}\ \frac{1}{2T\ \frac{P_s}{N_o}}\right]^{1/2} = \frac{1}{(2\rho)^{1/2}} \tag{2}$$

where $\frac{\pi^2}{8}$ is the degradation due to square wave reference, P_s/N_o is the signal power-to-noise density at the receiver AGC output and ρ is the effective SNR. The plot of equation (2) together with the measured performance is presented in Figure 5. This verifies that implemented digital processor closely approximates the maximum likelihood estimator performance.

For some purposes it is convenient to define the processor noise bandwidth. By comparing (2) with the phase variance at the output of a PLL, the equivalent single-sided noise bandwidth can be defined as

$$B_n = \left(\frac{\pi^2}{8}\right)^{1/2} \frac{1}{2T} \simeq \frac{1}{2T} \tag{3}$$

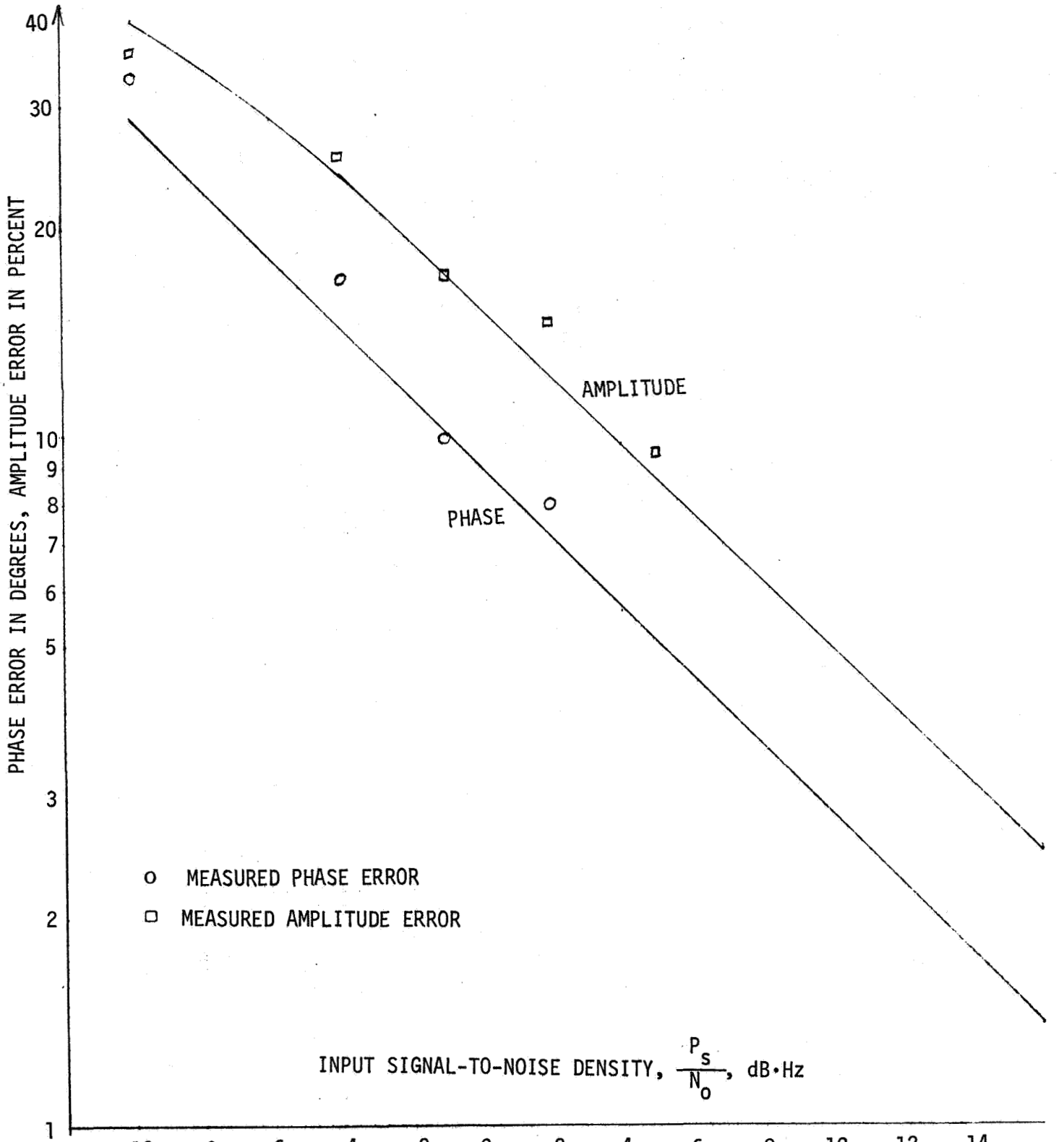

FIGURE 5. RMS NOISE ERRORS

For the nominal integration time of 25 seconds, we get a noise bandwidth of about 0.02 Hz. Note that with the digital implementation, the noise bandwidth can be reduced if necessary by simple increase of the integration time.

The maximum-likelihood amplitude estimator is equivalent to the ideal envelope detector used to detect sine wave in additive Gaussian noise[3]. Application of these well known envelope detector results to the processor shows that the mean of the estimated amplitude $\hat{A}$ is

$$\bar{\hat{A}} = \frac{\sqrt{\pi}}{2}\left(\frac{P_s}{\rho}\right)^{1/2}\left[(1+\rho)e^{-\rho/2}I_0(\rho/2)+\rho I_1(\rho/2)e^{-\rho/2}\right] \tag{4}$$

where I_0 and I_1 are the modified Bessel functions of order zero and one, respectively, and the variance is

$$\text{var}\,[\hat{A}] = P_s\left(1+\frac{1}{\rho}\right) - \left(\bar{\hat{A}}\right)^2 \tag{5}$$

The amplitude error defined as the standard deviation and expressed in percent of the mean is also given in Figure 5. It is interesting to point out that the theoretical amplitude error asymptotically approaches 52.3% with the decreasing ρ, however, the estimator is biased and the mean of the estimate increases due to the rectification of the noise.

IV. SYSTEM STABILITY

A stability analysis of the closed loop Conscan system can be simply performed because the system has an impulse controller and can be considered as quasi-static. For three spacecraft revolutions a "best" estimate of the desired precession direction is made. At the end of this period, the estimate is available, with no transient error in the ordinary sense associated with it. At this time, the momentum vector (which is normally fixed in inertial space and determines the basic pointing direction) is precessed a fixed amount in the estimated direction by a torque impulse from the thrusters. To determine stability, only the error in the estimate of the direction, along with the effect of this error on system behavior, need be considered.

When precessed, the resultant wobble is eventually damped out such that the spin axis and the momentum vector coincide. The wobble is bounded and since its major effect is to decrease the accuracy in the estimate of the precession direction, it can be treated as just another error source affecting the system ability to estimate phase. The two destabilizing factors are wobble growing without bound and precession at an improper angle such that the deadzone is not reached. With large pointing errors of the spin axis from the earth line, the spin axis can be precessed at any angle less than 90^{o} (phase angle < 90^{o}) and come closer to the earth in pointing. This is not true near the deadzone, however. In fact, the maximum allowable phase error angle is a function only of the deadzone and the precession step size. One can imagine that with a very small deadzone and a large step size, it would be impossible to reach within the deadzone at all.

Bias errors are more critical than random errors when the system approaches the deadzone. The system performance under the influence of introduced bias error can be predicted by a simple geometric approach. A sequence of precession steps from some arbitrary initial pointing error is performed geometrically until the deadzone is reached. Phase bias error can be introduced into each step and may be either constant, or a function of the pointing error as in the case of antenna errors. The number of precession steps required to reach the deadzone from some initial position as a function of the phase bias is a measure of the system stability. This number of steps is normalized to the ideal number (zero error). Since this normalized number is a measure of the fuel wasted, it is called the "gas usage ratio". A plot of the gas usage ratio versus phase bias is given in Figure 6. This plot is for the 1^{o} deadzone and 0.32^{o} (worst case) precession step size that would normally be used with the medium gain antenna. Since this figure is generated primarily from geometric considerations it also applies to the Conscan with the high gain antenna if the ratio of the deadzone to the step size is unchanged. Thus, Figure 6 is also directly applicable to the high gain antenna with 0.125^{o} deadzone and a 0.04^{o} step size.

Although the gas usage ratio was derived from geometric considerations only, the simulation results have shown surprising agreement with the analytical predictions. The error used for both the geometric estimate and the simulation was, however, an idealized constant bias, identical in both cases. In the next section, some simulation and test results with random errors (noise) are presented.

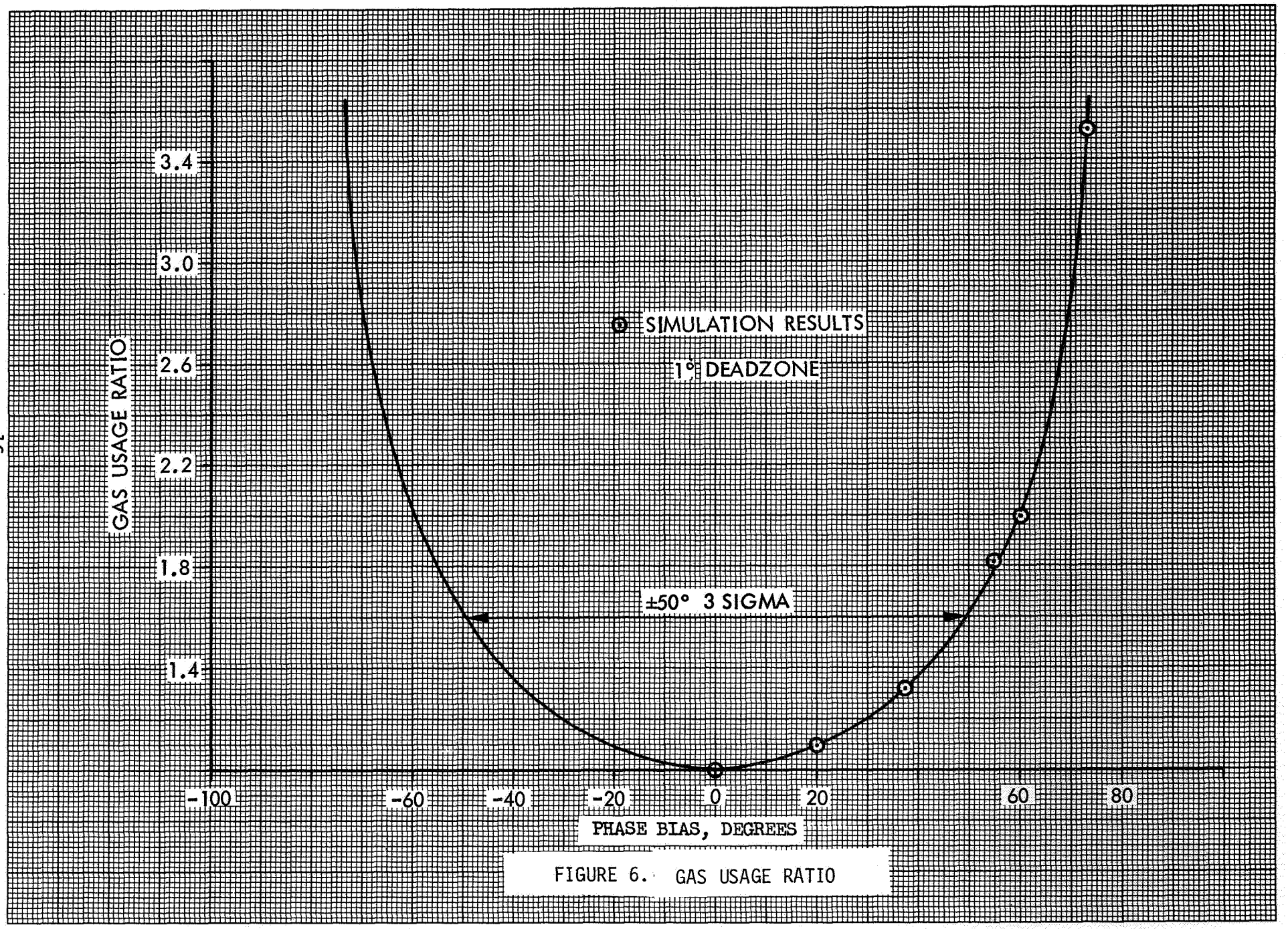

FIGURE 6. GAS USAGE RATIO

V. PERFORMANCE

The closed loop Conscan system performance is mainly determined by the phase and amplitude errors. As discussed in the previous section, the phase errors primarily determine the gas usage ratio. The amplitude errors establish how reliably Conscan can be terminated at the selected deadzone. In this section, open loop errors are described and related to the gas usage ratio and probability of Conscan termination. Closed loop simulation and test results are also presented to verify analysis. First, however, selection of the deadzone is discussed.

The Conscan system is required to point the spacecraft high gain antenna to within $\pm$ 0.5^{o} of the earth. In addition, this has to be accomplished with a minimum amount of propellant and minimum operational cost. Since the errors increase with decreasing pointing error angles, selection of a small deadzone (0.1^{o} for example) results in somewhat larger gas usage ratio. Selection of a large deadzone (0.4^{o} for instance) results in higher probability that Conscan is automatically terminated before the pointing error is reduced to 0.5^{o}. In this case, since the Conscan cannot be automatically initiated, a ground command to spacecraft has to be transmitted. At extreme distances, the propagation time is long (e.g., at Jupiter distance two-way propagation time is 1 hour and 40 minutes) and repeated attempts to achieve the desired 0.5^{o} pointing error may not be practical. Fortunately, for small errors, gas usage is not very sensitive to the choice of deadzone and it can be demonstrated that all requirements can be met with a deadzone ranging from 0.1^{o} to 0.4^{o}. For the high gain antenna a deadzone of 0.3^{o} has been selected.

The error budget for the engineering model spacecraft is presented in Table 1. Since many errors are approximately inversely proportional to the Conscan signal amplitude and the noise errors depend on the communications distance, this table is directly applicable to the pointing error of 0.3 degrees and the communications distance of 6 AU only. Note that a large number of error sources such as Deep Space Station (DSS) antenna gain variation, transmitter amplitude modulation, spacecraft antenna even harmonics, polarization, ellipticity and frequency reference phase jitter have been computed and found to be negligible.

TABLE 1. CONSCAN ERROR BUDGET FOR THE HIGH GAIN ANTENNA
(0.3^{o} Pointing Error Angle)

	Phase Error in Degrees		Amplitude Error in Percent		COMMENTS
	1 Sigma	3 Sigma or Peak	1 Sigma	3 Sigma or Peak	
Antenna Measurement and Antenna Pattern Ripple	1	3	1.1	3.3	Estimates based on measurement accuracy analysis and large number of independent measurements
Antenna Third Harmonic	0.6	0.8	0.9	1.3	Based on measured interference-to-signal amplitude ratio of 3.8%
Antenna Mechanical Alignment	2.9	8.6	4.2	14.2	Based on predicted 3 sigma misalignment in the YZ plane of 0.13^{o} and in the XZ plane of 0.15^{o}.
Thermal Noise	1.5	4.5	2.5	7.5	Based on 85 ft. 10 kW DSS, 6 AU distance and results of Section III.
Receiver Gain Factor Measurement	-	-	1.3	4	Estimates based on repeated measurements
Processor Computation	1.8	2.5	4.3	6	Computed and measured
Spin Rate Variation	1.6	2.8	0.2	0.3	Variation in AGC loop and processor input filter response due to $\pm$ 20% variation in conscan signal frequency.
Wobble	1.4	2	2.5	3.5	Based on Appendix A
TOTAL (Random)	4.5	11	7.25	18.4	Total error is the root-sum-square of individual errors
Antenna Phase Variation (Bias)	-	5.3	-	-	Based on measurements.

In general, it can be verified that the individual errors are uncorrelated. Still, the rigorous computation and interpretation of the total error is complicated by the fact that the individual sources do not have the same statistical distributions and some are slowly varying relative to the Conscan time. For mathematical tractability, however, this problem has been neglected and the total random error is computed by root-sum-squaring all individual sources.

The worst case gas usage ratio can now be determined by treating the computed total 3 sigma phase error (3 sigma random & bias in Table 1) as a bias. Under this assumption, Figure 6 can be used and the three sigma gas usage ratio corresponding to a phase error of 16.3 degrees is found to be less than 1.1. Thus, the amount of gas wasted due to the imperfect phase measurement is essentially negligible.

The total amplitude error establishes how reliably Conscan can be terminated at the selected deadzone. Since the Conscan signal amplitude is approximately proportional to the pointing error angle, these amplitude errors can be converted to deadzone errors expressed in degrees which we will refer to as pointing accuracy. For example, corresponding to the 7.25% total amplitude error, for the nominal deadzone of 0.3 degrees, the one-sigma pointing accuracy is 0.022 degrees. In Figure 7, the predicted pointing accuracy for other deadzones is plotted. Using results of Appendix B, it can be shown that even for a 0.1 degree deadzone, Conscan operation will be terminated between pointing error angles of $0.1 - \Delta\varepsilon$ and $0.1 + \Delta\varepsilon$ with probability of 0.99.

Verification of the system performance has been performed both by an extensive simulation and by closed loop tests. This simulation and testing included both nominal and worst case unit models and flight conditions. For example, tests with worst case antenna ripple, mechanical misalignment and spin rate variations have been included. In all cases, Conscan operation with increased gas usage ratio was possible. Next, some typical simulation and test results are described.

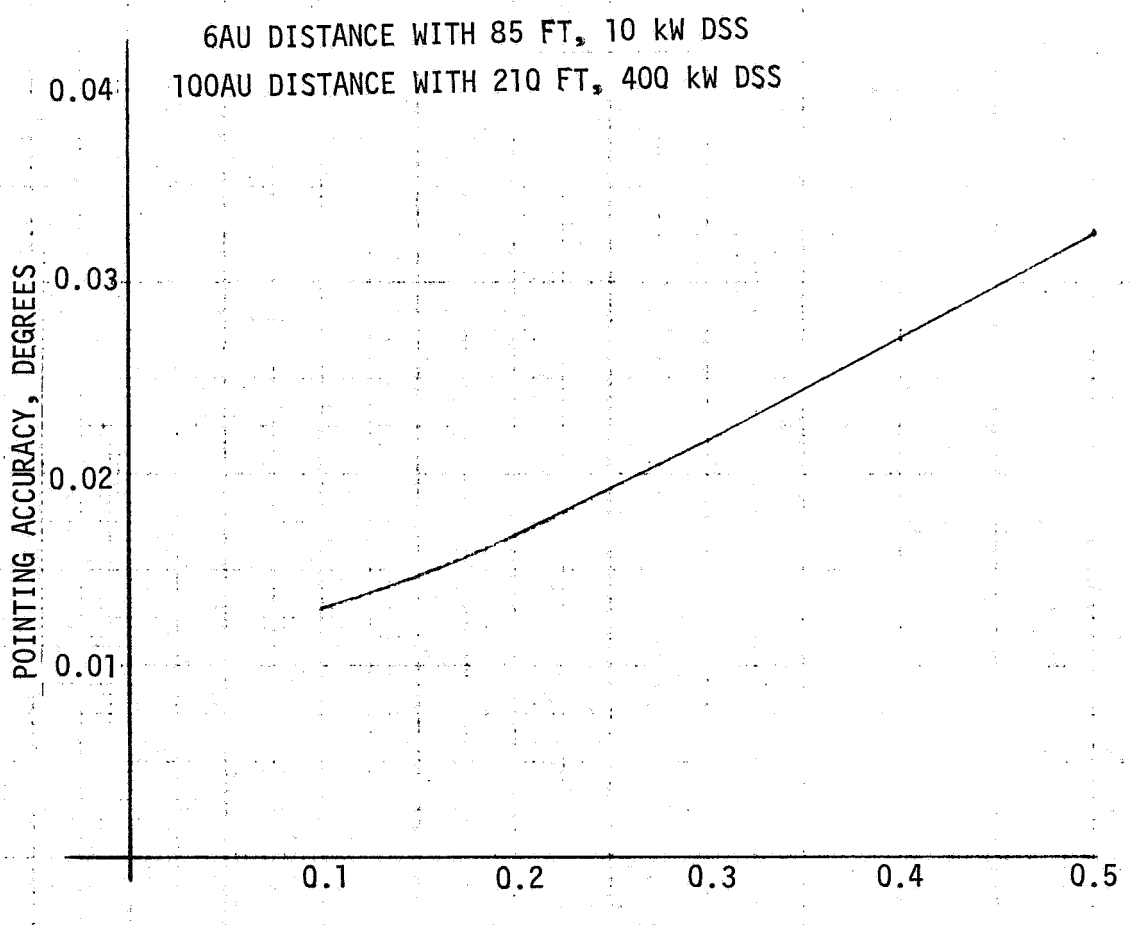

FIGURE 7. CONSCAN POINTING ACCURACY

Figure 8 is a simulation results and illustrates spin axis precession with superimposed wobble. It presents the "Conscan trajectory" which is a projection of the spin axis on a plane perpendicular to the earth line. The circle represent wobble and confirms the existance of two wobble frequencies. The almost ideal straight line path is in agreement with the simulation conditions since idealized antenna, receiver AGC and signal processor models were used. The primary objective of the simulation and the closed loop tests was to verify the implementation concept.

The elliptical Conscan trajectory shown in Figure 9 illustrates the effect of a bias error. It shows that the number of steps to reach the deadzone starting from an initial position of 5^{o} increases and results in propellant gas waste. The 36^{o} phase bias was intentionally inserted to verify system stability. A phase error of this magnitude is not expected for any flight condition.

In the closed loop test of the system, the engineering models of the receiver, signal processor, and the spin period sector generator were used. The spacecraft dynamics, antenna and the sun sensor were simulated on an analog computer. A typical test trajectory is shown in Figure 10. The conditions under which this trajectory was obtained correspond closely to the actual flight conditions with the exception of larger communication distance (15 AU), and the fact that the antenna mechanical alignment and antenna measurement errors were not simulated. The trajectory is a straight line, indicating absence of phase bias and the negligible effect of random (noise) errors. The large wobble amplitude at the beginning of the trajectory is due to test implementation characteristics and will not exist during the flight. The final trajectory, Figure 11, shows the effect of extremely large phase bias. While the deadzone was still reached without difficulty, the gas usage ratio increased to 1.7.

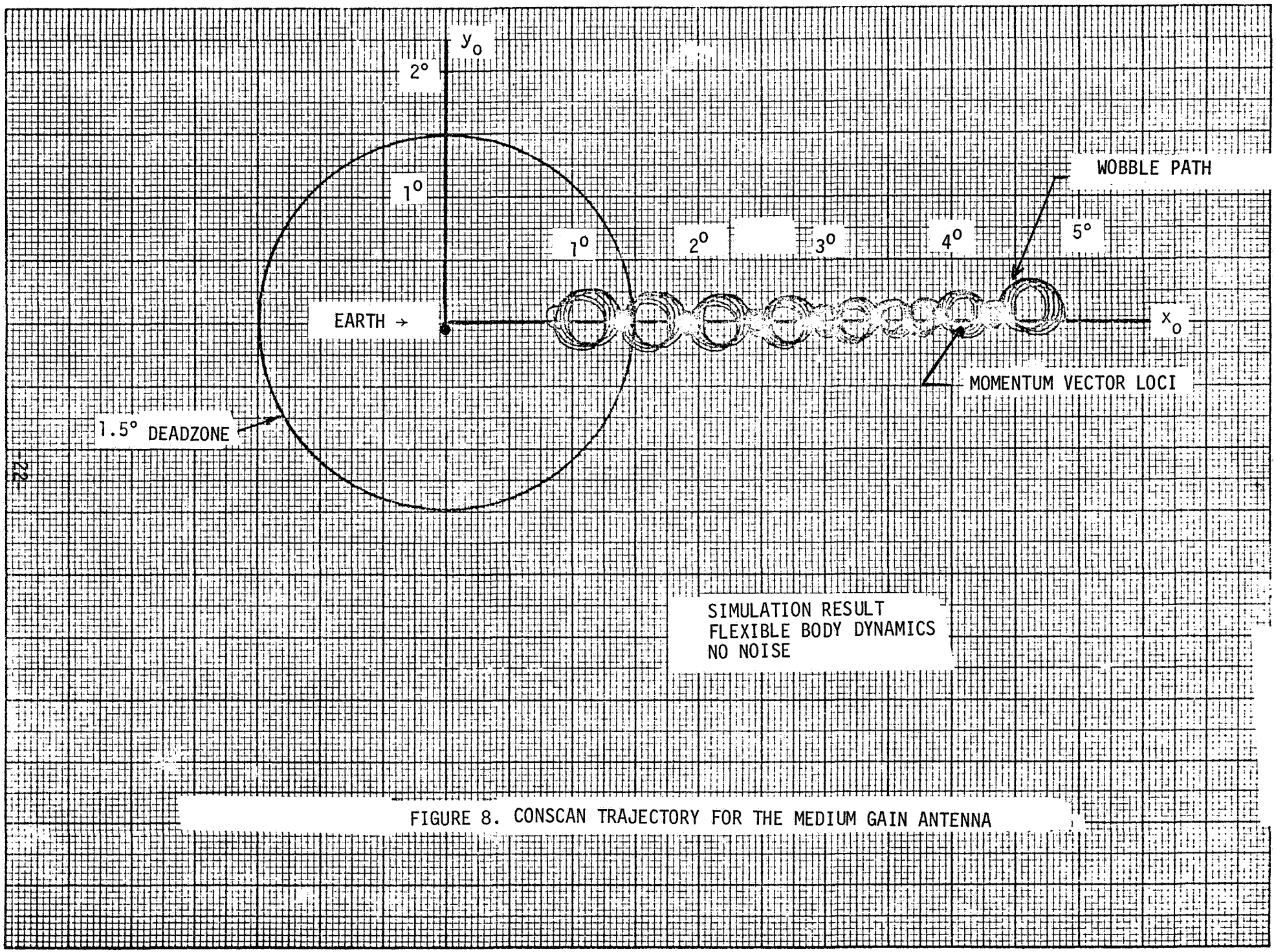

FIGURE 8. CONSCAN TRAJECTORY FOR THE MEDIUM GAIN ANTENNA

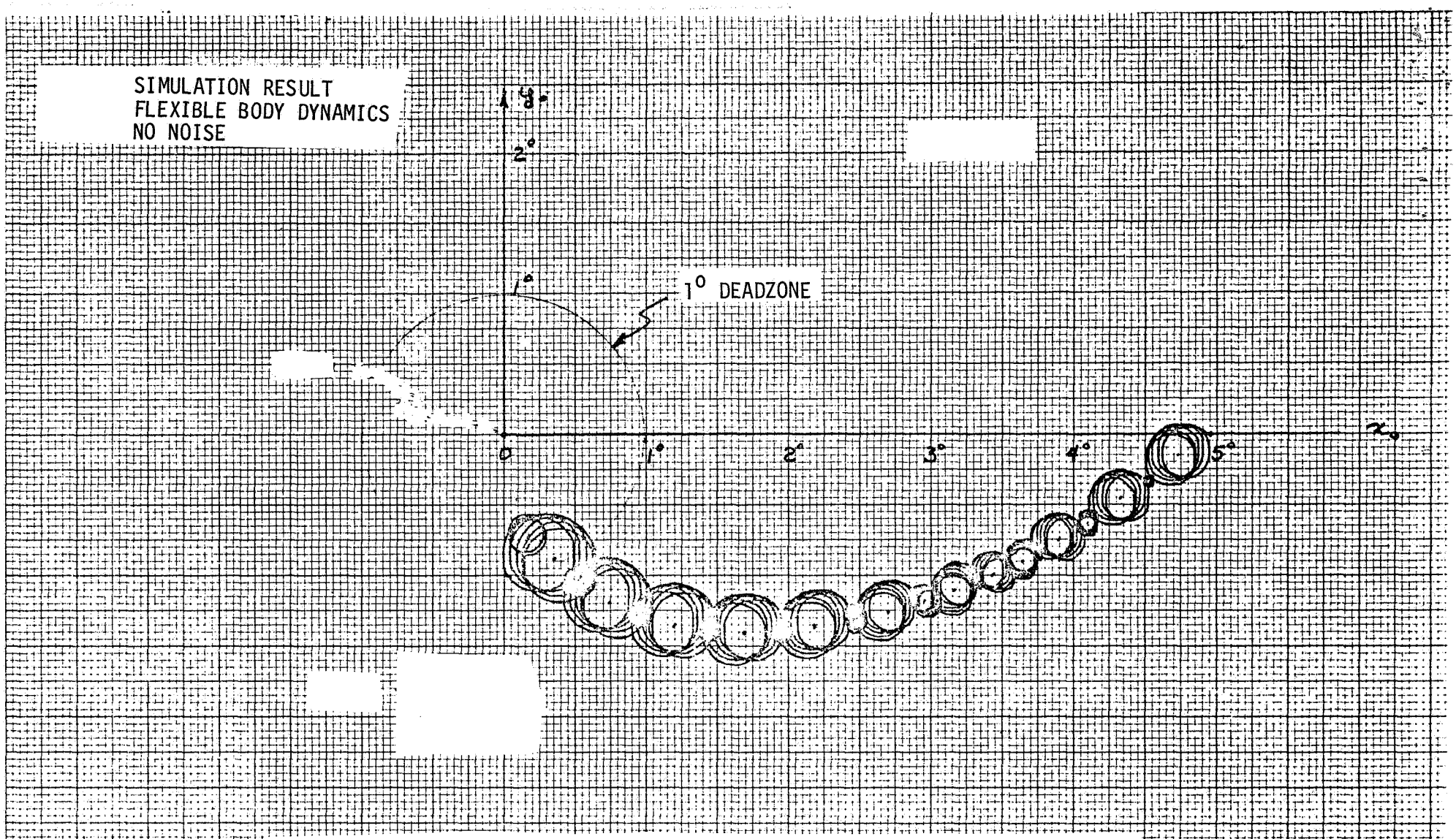

FIGURE 9. CONSCAN TRAJECTORY FOR MEDIUM GAIN ANTENNA WITH 36° BIAS

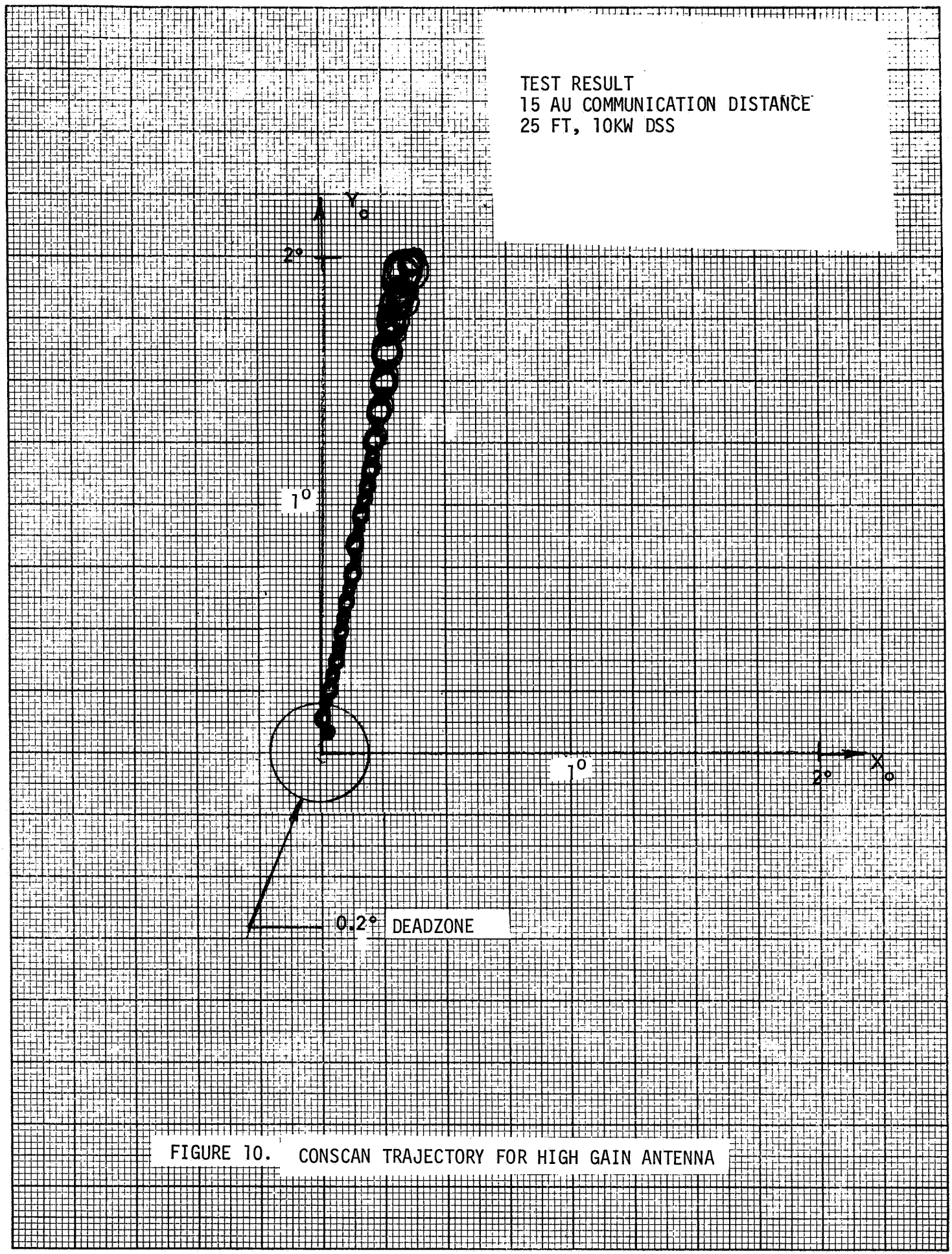

FIGURE 10. CONSCAN TRAJECTORY FOR HIGH GAIN ANTENNA

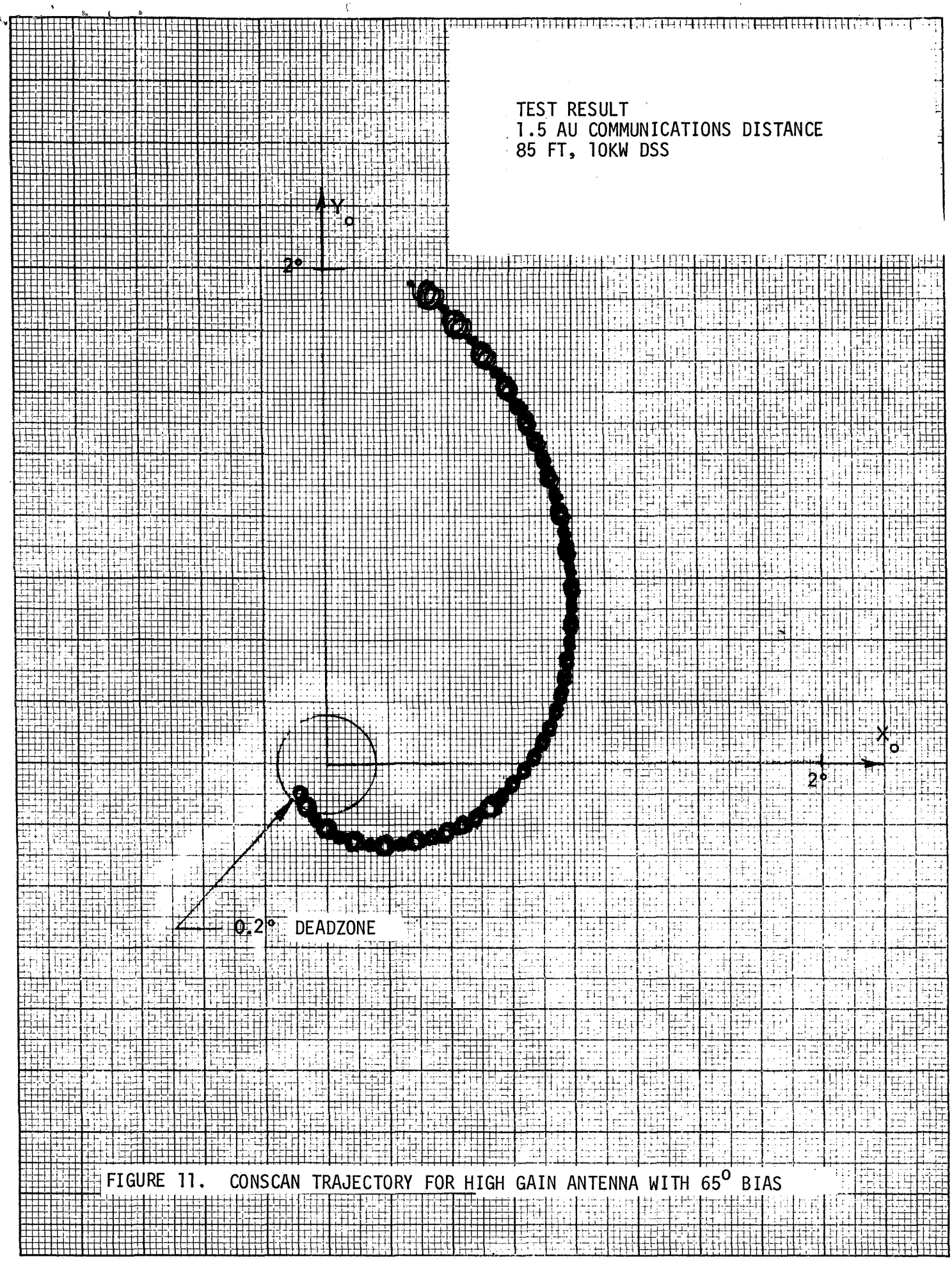

FIGURE 11. CONSCAN TRAJECTORY FOR HIGH GAIN ANTENNA WITH 65° BIAS

CONCLUSION

We have shown that for the spin stabilized spacecraft, the Conscan system described here can be very simply implemented. We have also presented analytical and experimental results which verify that the 9-foot spacecraft antenna can be accurately pointed at the earth (0.3 degree deadzone).

The present Conscan system, with minor modifications, can be used for Advanced Pioneer missions to other planets. To improve communications performance, Advanced Pioneer might employ larger deployable antennas and use X-band frequency on the downlink and, therefore, require more accurate pointing. Preliminary analysis indicates that Conscan system performance can be easily improved to meet this more stringent pointing accuracy requirement.

ACKNOWLEDGEMENT

The results described here represent an achievement of many individuals from the TRW Systems Group Electronic and Space Vehicle Divisions. Their contribution in formulating concept, system design, implementation, and analysis is hereby acknowledged.

APPENDIX A

SPACECRAFT DYNAMICS

In this appendix, a simplified description of the dynamic behavior of the spacecraft is presented. The implications of this behavior on the Conscan design are discussed.

The basic equations describing the motion of the spacecraft are the Euler equations:

$$\dot{\omega}_x = \frac{I_y - I_z}{I_x} \omega_y \omega_z + \frac{T_x}{I_x}$$

$$\dot{\omega}_y = \frac{I_z - I_x}{I_y} \omega_x \omega_z + \frac{T_y}{I_y}$$

$$\dot{\omega}_z = \frac{I_x - I_y}{I_z} \omega_x \omega_y + \frac{T_z}{I_z}$$

where

$I_{x,y,z}$ = spacecraft principal moment of inertia about x, y or z axis.

$T_{x,y,z}$ = torque about x, y or z axis

$\omega_{x,y,z}$ = angular velocity about x, y or z axis

For brevity in this paper, these equations do not include a number of effects which have been considered, namely, flexible body effects and damping by the wobble damper.

The above general equations can be simplified for the Pioneer spacecraft. The spacecraft configuration is such that the thrusters only apply a torque about the x axis, thus $T_z = T_y = 0$. Spin rate changes during precession are negligible such that $\omega_z = \omega_s$, a constant. No other simplification can be made without hiding some important effects.

The precession control is obtained by firing the thrusters at the appropriate time to precess the spin axis (z_b) in the desired direction. When this occurs, the momentum vector moves to the new position and the spacecraft wobbles about this position as described by these equations. The proper firing time is computed by the signal processor which detects the earth spin axis plane and issues a signal when the thrusters are in the proper position.

After the appropriate introduction of kinematics and Euler angles, these equations can be solved by ordinary Laplace transforms. The spin axis is projected onto a fixed inertial plane (called the δ plane) containing the path of the momentum vector. The projection of the spin axis onto the δ plane is given by the solution of the Euler equations. This result describes the wobble motion and is given by:

$$\delta(t) = \frac{k_y - 1}{\omega_s^2(k^2 - 1)} \frac{2T_x}{I_x}(N) \sin\frac{\xi}{2}$$

$$+ \frac{T_x \sin k\xi/2\pi \sin Nk\pi r}{I_x k k_x \omega_s^2 \sin k\pi r} - \frac{k_x + k}{k + 1} \sin[(1 + k)\,\omega_s t + \phi_1]$$

$$+ \frac{k - k_x}{k - 1} \sin[(1 - k)\,\omega_s t + \phi_2]$$

where

$$k_x = \frac{I_z - I_y}{I_x},\quad k_y = \frac{I_z - I_x}{I_y},\quad k = k_x k_y = 0.85,$$

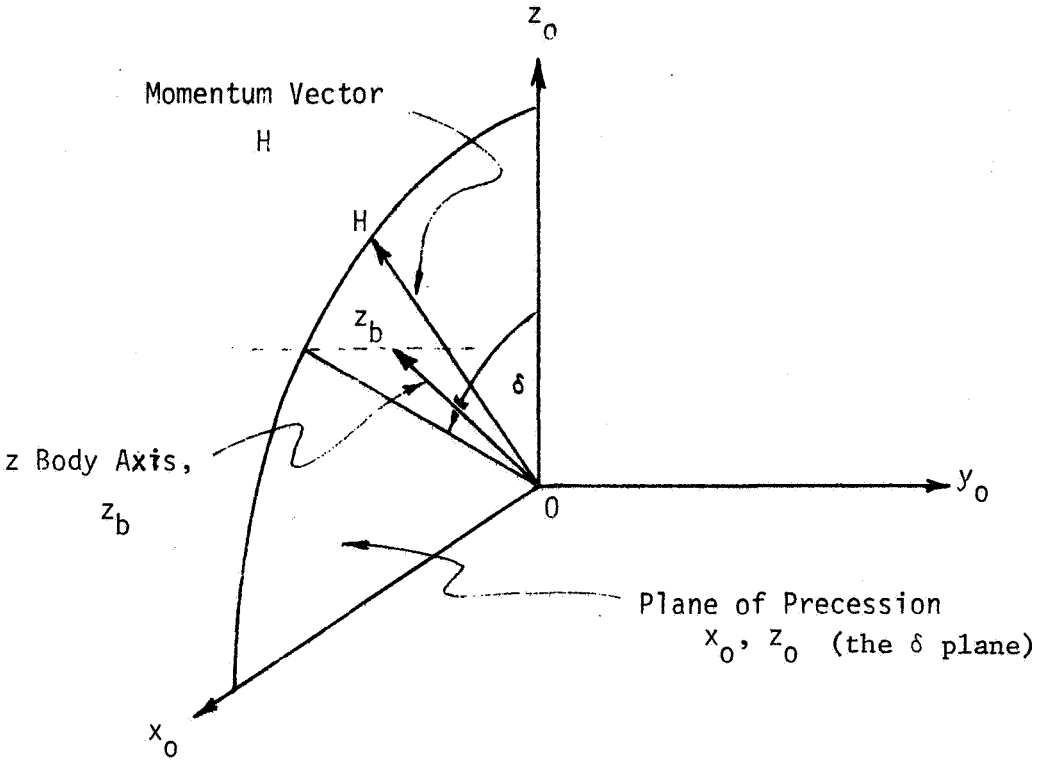

Figure A-1. Geometry of the Spin Axis and the Momentum Vector Path.

T_x = torque applied = 8.5 ft lb

ξ = angular width of thruster pulse fired - 3.6^o for medium gain antenna pulses

ω_s = the vehicle spin rate = 0.503 rad/sec

r = number of vehicle revolutions between thruster firings = 3

All of the above are constants. The only remaining terms are N, the number of pulses fired, phase angles ϕ_1 and ϕ_2 which depend on initial conditions, and time, t. The interpretation of the solution is now simplified.

The first term in the solution is a constant multiple of N. That is, each pulse fired causes the centroid of the angular position (the momentum vector) to increase by a constant amount equal to the precession step size. This term nominally describes the position of the momentum vector. The second term in the solution is sinusoidal, and describes the wobble motion about the momentum vector. Damping of wobble is not included in this simplified solution. If it was included it would show that the wobble eventually dies out after the pulse firing is terminated. Note that two wobble frequencies occur, $(1 + k)\omega_s$ and $(1-k)^{\omega_s}$. The first of these is the larger in amplitude and dominates the appearance of the wobble.

The term outside the brackets is of great importance for Conscan since it contains the term sin $k\pi r$ in its denominator. For some combinations of k and r, this term can be zero which implies that the wobble can grow without bound if pulsed enough - note the term sin $Nk\pi r$ in the numerator. In the Conscan processor, it is desirable to compute the phase and amplitude signals for a relatively long time (multiple of spin period) to improve the accuracy. A tradeoff is made in the selection of r between wobble interference with the Conscan signal and the processor noise bandwidth described previously. The wobble amplitude can be very large since for large r, the term sin $k\pi r$ is very sensitive to small changes in k. If $(\sin k\pi r)^{-1}$ is plotted for different values of k as a function of r, it is seen that local minima occur as shown in Figure A-2. For k = 0.87, the minima are at r = 3.7, 11.5, 10.5, etc. For k = 0.85, the minima occur at r = 3.3, 10, 16.6,... Since it was predicted that k would be about 0.85, the value r = 3 was selected for the optimum interval between pulse firings.

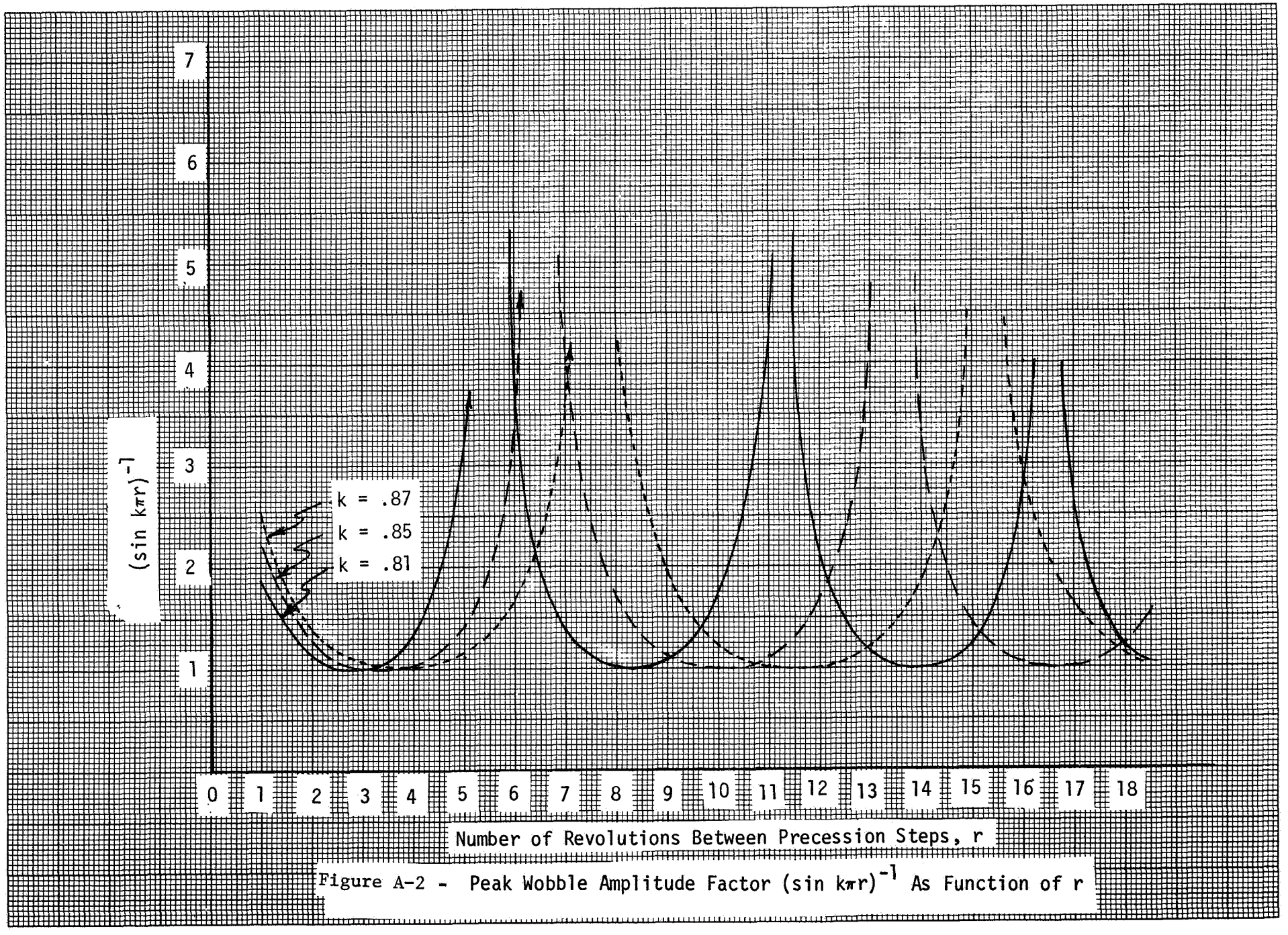

Figure A-2 - Peak Wobble Amplitude Factor $(\sin k\pi r)^{-1}$ As Function of r

APPENDIX B

CONSCAN TERMINATION PROBABILITY

Assuming that the amplitude measurements from pulse-to-pulse are uncorrelated, the probability that Conscan has not been terminated $P_c(\varepsilon)$, at pointing angle, ε, can be approximated by the cumulative probability

$$P_c(\varepsilon) = \prod_{n=0}^{N} \left\{ 1 - P_T[\varepsilon_i - (\Delta\varepsilon)n] \right\}$$

where

$N = \dfrac{\varepsilon_i - \varepsilon}{\Delta\varepsilon}$ = number of precession steps

ε_i = Initial pointing angle

$(\Delta\varepsilon)$ = Precession step size

$P_T(\alpha)$ is the single shot probability of crossing threshold at angle α. Since the total error is a sum of many statistically independent variables, using Central Limit Theorem, it can be justified that the sum has a Gaussian distribution. Therefore, $P_T(\alpha)$ if found from

where

$$X = \frac{A_T - \bar{\hat{A}}}{\Delta A}$$

A_T = threshold setting

$\bar{\hat{A}}$ = signal amplitude at the threshold detector input

ΔA = total 1 sigma error at the threshold detector input presented in Table 1

Using the above expressions, it can be shown that even for a deadzone of 0.1 degrees the Conscan operation will be terminated between pointing error angles of 0.1 $-\Delta\varepsilon$ and 0.1 + $\Delta\varepsilon$ with probability of 0.99.

REFERENCES

1. D. Slepian, "Estimation of Signal Parameters in the Presence of Noise", Trans. IRE, PGIT-3, 68, March 1954.

2. D. D. Carpenter, "The Problem of Estimating the Unknown Phase of a Sine Wave Signal in Gaussian Noise", unpublished TRW Systems Group Report.

3. S. O. Rice, "Mathematical Analysis of Random Noise", Bell Systems Technical Journal, Vol. 24, 1948.